Journal of Medicinal Chemistry

Article

pubs.acs.org/jmc

Lead Optimization Studies of Cinnamic Amide EP2 Antagonists

Thota Ganesh,* Jianxiong Jiang, Myung-Soon Yang, and Ray Dingledine

Department of Pharmacology, School of Medicine, Emory University, 1510 Clifton Road, Atlanta, Georgia 30322, United States

Supporting Information

ABSTRACT: Prostanoid receptor EP2 can play a proinflammatory role, exacerbating disease pathology in a variety of central nervous system and peripheral diseases. A highly selective EP2 antagonist could be useful as a drug to mitigate the inflammatory consequences of EP2 activation. We recently identified a cinnamic amide class of EP2 antagonists. The lead compound in this class (**5d**) displays anti-inflammatory and neuroprotective actions. However, this compound exhibited moderate selectivity to EP2 over the DP1 prostanoid receptor (~10-fold) and low aqueous solubility. We now report compounds that display up to 180-fold selectivity against DP1 and up to 9-fold higher aqueous solubility than our previous lead. The newly developed compounds also display higher selectivity against EP4 and IP receptors and a comparable plasma pharmacokinetics. Thus, these compounds are useful for proof of concept studies in a variety of models where EP2 activation is playing a deleterious role.

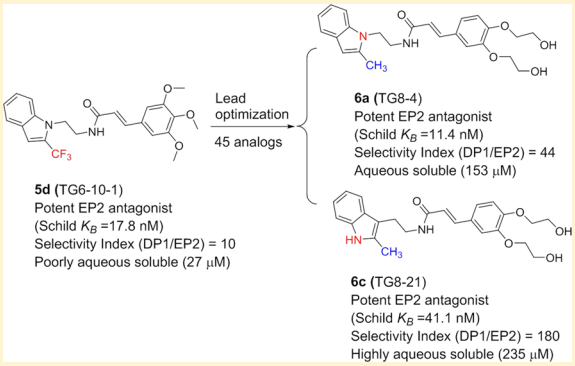

INTRODUCTION

Inflammation plays a pathogenic role in a variety of acute and chronic neurodegenerative diseases such as status epilepticus (SE), epilepsy, amyotrophic lateral sclerosis (ALS), Alzheimer's disease (AD), Parkinson's disease (PD), and traumatic brain injury (TBI).[1−8] Cyclooxygenase 2 (COX-2) is induced during and after brain injury and is a major contributor to the inflammation and disease progression in a variety of central nervous system (CNS) diseases.[9−12] COX-2 inhibitors have been widely explored for suppression of pain and inflammation in variety of peripheral diseases, for example, in patients with arthritis.[13,14] However, COX-2 inhibitors cause adverse cardiovascular effects by reducing activation of a downstream prostanoid receptor subtype IP.[15−18] As a result, two COX-2 inhibitors, rofecoxib (Vioxx) and valdecoxib (Bextra), were withdrawn from the U.S. market. Moreover, it is not yet clear that COX-2 inhibitors could provide a benefit to patients with chronic inflammatory neurodegenerative diseases such as epilepsy and AD.[19−26] Thus, future anti-inflammatory therapy should be targeted through a specific proinflammatory prostanoid synthase or receptor to blunt the inflammation and neuropathology in CNS diseases rather than to block the entire COX-2 signaling.

COX-2 catalyzes the synthesis of prostaglandin-H_2 (PGH_2) from arachidonic acid, which is transformed into five prostanoids, PGD_2, PGE_2, PGF_2, PGI_2 and TXA_2, by cell specific synthases. These prostanoids activate nine receptors, DP1, DP2, EP1, EP2, EP3, EP4, FP, IP, and TP. Each of these receptors can play protective as well as harmful roles in a variety of CNS and peripheral pathophysiologies.[27−29] EP2 receptor has emerged as an important biological target for drug discovery to treat a variety of CNS and peripheral diseases.[30,31] When activated by PGE_2, EP2 stimulates adenylate cyclase resulting in elevation of cytoplasmic cAMP concentration, which initiates downstream events mediated by protein kinase A (PKA)[32,33] or exchange protein activated by cAMP (Epac).[34−36]

The EP2 receptor is widely expressed in both neurons and glia in the brain and plays a "yin−yang" nature of protective as well as deleterious role.[31] For example, in some chronic neurodegenerative disease models, EP2 activation appears to promote inflammation and neurotoxicity. Deletion of the EP2 receptor reduces oxidative damage and amyloid-β burden in a mouse model of AD.[37] EP2 deletion also attenuates neurotoxicity by α-synuclein aggregation in mouse model of PD.[38] Moreover, EP2 deletion improves motor strengths and the survival of the ALS mouse.[39] Furthermore, mice lacking EP2 receptors have shown less cerebral oxidative damage produced by the activation of innate immunity.[40] In vitro, microglia cultures from mice lacking EP2 have shown enhanced amyloid-β phagocytosis and are less sensitive to amyloid-β induced neurotoxicity.[41] Despite a wealth of information available from EP2 gene knockout studies, results from pharmacological inhibition of EP2 are limited because the antagonists for EP2 receptors have only been created recently by Pfizer[42] and us.[43] Earlier, we reported identification of a cinnamic amide class of EP2 antagonists by using a high-throughput screening method.[43] A limited structure−activity relationship study (SAR) concluded that this class of compounds displays high potency to EP2 receptor but moderate selectivity to EP2 over another prostanoid receptor, DP1. The lead compound in this class, **5d** (aka TG6-10-1), displays about 10-fold selectivity to EP2 over DP1 and poor aqueous solubility (27 μM). However,

Received: January 13, 2014
Published: April 28, 2014

5d demonstrated robust neuroprotective and anti-inflammatory effects in a pilocarpine model of status epilepticus when administered in three doses beginning 4 h after mice entered into status epilepticus.[44] A key to advance this class of compounds for preclinical studies in a variety of neurodegenerative disease models is to improve their EP2 selectivity, aqueous solubility, and in vivo pharmacokinetics. In the present study we report the synthesis of 45 new analogues and their structure–activity relationships and show that improvements are made in terms of selectivity, solubility, and metabolic stability in liver microsomes. Two compounds, **6a** and **6c**, display about 4- to 18-fold higher selectivity against DP1 receptor and 5- to 8-fold higher aqueous solubility than the previous best compound **5d**.

RESULTS AND DISCUSSION

First Generation Cinnamic Amide EP2 Antagonists Show Poor Aqueous Solubility, Poor in Vitro Liver Microsomal Stability, and Moderate Plasma Half-Life. We previously synthesized 27 compounds around initial high-throughput screening hit **5a** (aka TG4-155) (Figure 1) for

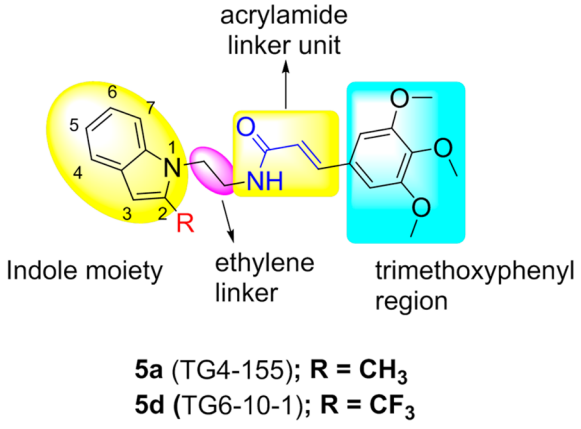

Figure 1. Optimization strategy. Structures of representative first generation EP2 antagonists. Regions marked are explored for SAR study.

structure–activity relationship study. Several derivatives from this set showed potent EP2 inhibition with Schild K_B values at the low nanomolar level, and they also displayed excellent selectivity against EP4 and β-AR receptors.[43] To examine the druglike properties within the class, 10 potent compounds (EP2 Schild K_B < 20 nM) were selected and subjected to metabolic stability in microsomal fractions of mouse and human liver at two different concentrations (1 and 10 μM). A majority of these compounds were found to be labile in these liver fractions with <15 min half-life at 10 μM concentration[43] except one compound **5d**, which showed >15 min half-life in mouse and human liver microsomes at 10 μM (Table 3). Moreover, compound **5d** showed improved brain-to-plasma ratio (1.7) and plasma half-life (1.7 h) in a pharmacokinetic (PK) study in C57BL/6 mice, in comparison to initial hit compound **5a**.[44] Although **5d** has been used for initial proof of concept studies, the plasma half-life should be improved for testing in a wider variety of preclinical models.

The structural identity among the prostanoid receptor family is very limited. EP1, EP2, EP3, and EP4 share a common endogenous ligand PGE_2 for their activation, but they only share 20–30% structural homology.[45] In contrast, EP2 is more homologous to DP1 (44%) and IP receptors (40%).[45] Earlier, compounds **5a** and **5d** were tested against other prostanoid receptors. Although they displayed high selectivity to EP2 over EP1, EP3, EP4, FP, IP, and TP receptors, they showed only moderate selectivity (~10-fold) to DP1 receptor.[44,46] None of the earlier set of 27 compounds were more selective over DP1 than **5a** and **5d** (not shown). Furthermore, compounds **5a** and **5d** displayed low aqueous solubility (45 and 27 μM, respectively) (Table 1). Thus, our initial goal was to identify compounds with enhanced selectivity and aqueous solubility.

Synthesis and Further Structure–Activity Relationship Study on Cinnamic Amide Analogues. The scaffold **5a** (Figure 1) possess four obvious sites for structural modification: (i) trimethoxyphenyl group, (ii) acrylamide moiety, (iii) ethylene linker, (iv) a methyl group on the indole ring. Earlier, we had designed a compound **5d** with CF_3 in place of CH_3 on the indole ring, with a premise that the fluorine atom(s) often enhances ADME properties.[47] Indeed, this transformation enhanced metabolic stability (Table 3) and brain and plasma PK properties.[44] However, the CF_3 analogue (**5d**) was about 7-fold less potent for EP2 in comparison to the CH_3 analogue **5a** (Table 2). In the present study, to examine whether three methoxyl groups on the phenyl ring are important for bioactivity, we have synthesized several derivatives that have reduced number of methoxyl groups or were completely substituted with other substituents as shown in Scheme 1. The synthesis is carried out starting from

Scheme 1. Synthesis of First Generation 1-Indole Cinnamic Amide EP2 Antagonists[a]

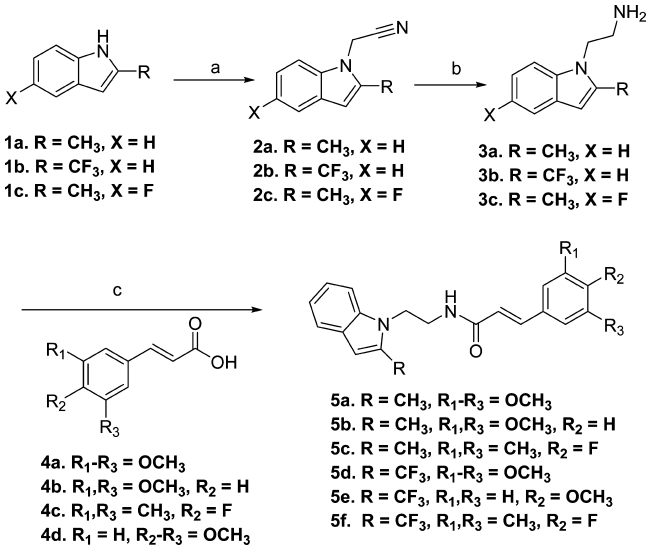

[a]Reagents and conditions: (a) NaH, bromoacetonitrile, DMF, 75%; (b) lithium aluminum hydride (LAH), tetrahydrofuran (THF), 32–57%; (c) cinnamic acid drivative (**4**), 1-ethyl-3-(3-dimethylaminopropyl)carbodiimide hydrochloride (EDCI), dimethylaminopyridine (DMAP), CH_2Cl_2, 75–80%.

commercially available 2-methylindole or 2-trifluoromethylindoles (**1a–c**), which on treatment with bromoacetonitrile provided intermediates (**2a–c**), which then were subjected to lithium aluminum hydride to reduce cyanide to amine, providing advanced intermediates **3a–c** in poor to moderate yields. In an effort to improve the yield of amines, we explored other methods of cyanide reduction using a variety of reducing

dx.doi.org/10.1021/jm5000672 | J. Med. Chem. 2014, 57, 4173–4184

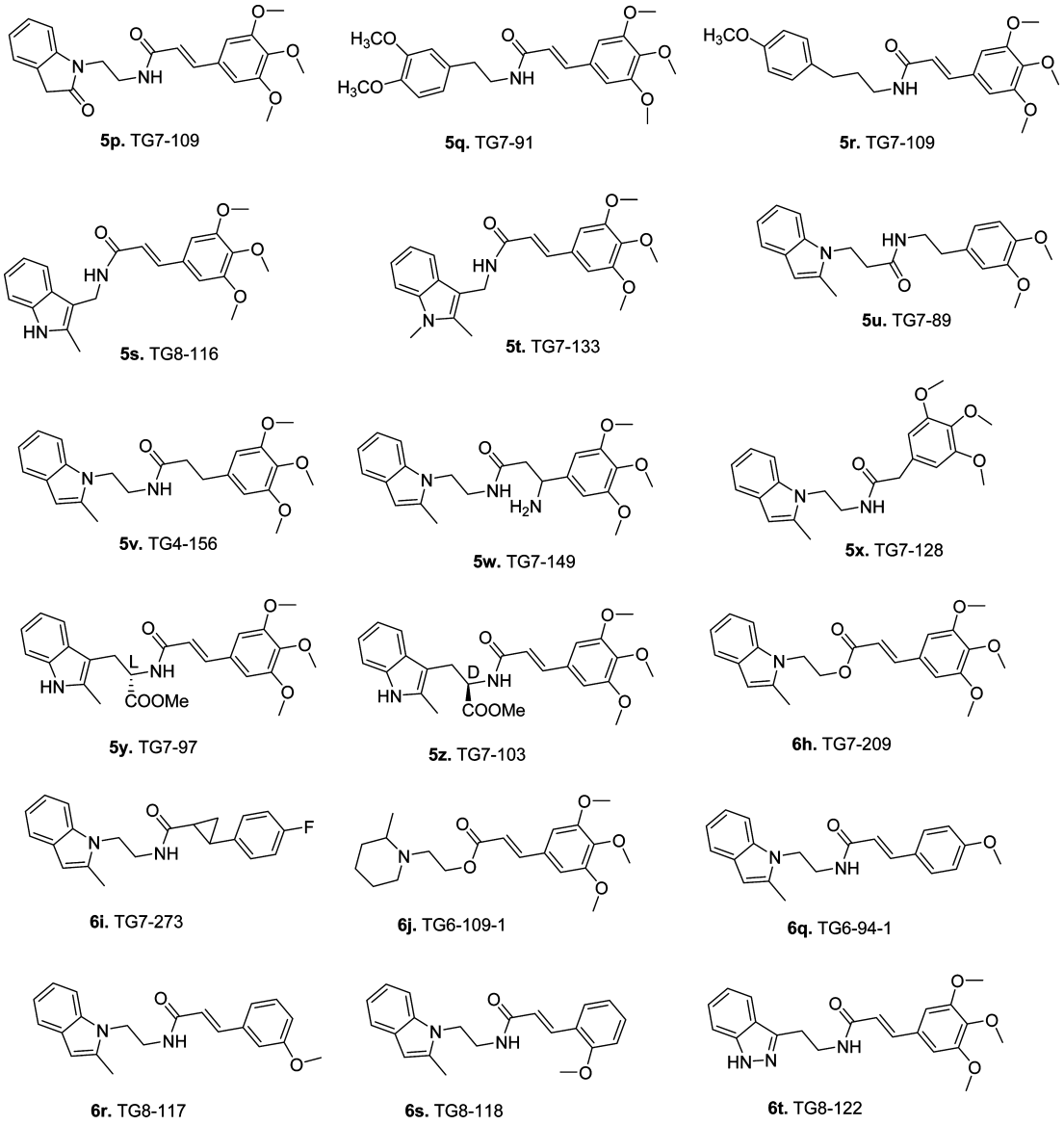

Figure 2. List of additional active/inactive first generation cinnamic amide derivatives synthesized and used for SAR study.

agents (see Supporting Information Table S1). These methods provided limited success, and they often resulted in an unwanted indole-dimer product as a major constituent. The classical lithium aluminum hydride (LAH) reduction method provided only 32−57% yield of the required amine products (Supporting Information Table S1 and discussion in the Supporting Information text). These amines were coupled to 3,4,5-trimethoxycinnamic acid derivatives (**4a**−**c**) to provide final products (**5a**−**f**) (Scheme 1). As shown in Table 1, newly synthesized derivatives are tested by using a cAMP-derived TR-FRET assay[48] at single concentration (1 μM) to observe a rightward shift of PGE_2 (an EP2 agonist) concentration−response curve in a C6G cell line that overexpresses human EP2 receptors (see Experimental Methods for details). From this a Schild K_B value (a concentration required to cause a 2-fold rightward shift of agonist EC_{50}) is calculated assuming a Schild slope of 1.07, which is the mean slope determined from four concentration (0.1, 0.3, 1, and 3 μM) Schild plots carried out on a dozen compounds in this series. A similar procedure is carried out with human DP1 receptors at a single compound concentration of 10 μM and used to rank-order the analogues based on EP2 potency and selectivity against DP1.

The structure−activity relationship (SAR) study indicates a 3,5-dimethoxycinnamic amide derivative (**5b**) and a compound in which three methoxyls are substituted with two methyl groups and a fluorine (**5c**) display similar EP2 potency, in comparison to **5a**. These derivatives show improved selectivity against DP1 (**5b** displays 24-fold, and **5c** displays 60-fold) (Table 1). We have earlier shown that a single methoxycinnamic amide derivative (**6q**, Figure 2) exhibited 7-fold less potency (K_B = 16.5 nM) on EP2 in comparison to parent **5a**.[43] We now synthesized compounds with single methoxyl group at ortho and meta positions. The *m*-methoxy derivative (**6r**, Figure 2) is about 2-fold less potent than *p*-methoxy derivative (**6q**), but the *o*-methoxy derivative (**6s**, Figure 2) displayed a similar potency to **6q** (Table 1). All of these single methoxy derivatives are about 5- to 12-fold less potent than a trimethoxy derivative (**5a**) or a dimethoxy derivative (**5b**). Similar exercises on CF_3 analogue **5d**, for example, substitution of three methoxyls with a single methoxyl group (**5e**) or two methyl groups and a fluorine (**5f**), reduced the EP2 activity by 16-fold

dx.doi.org/10.1021/jm5000672 | J. Med. Chem. 2014, 57, 4173−4184

in comparison to **5d** (Table 1). Taken together, these results indicate that three methoxyl groups on the phenyl ring are not absolutely essential for EP2 activity.

In parallel to indole-1 derivatives (Scheme 1), we also explored synthesis of several indole-3 derivatives (Scheme 2) as positional isomers. As shown in Scheme 2, commercially available 2-(2-methyl-1*H*-indol-3-yl)ethanamines (**3k**, **l**) were coupled to cinnamic acid derivatives (**4a**,**c**,**d**) to synthesize compounds **5g**−**j**. Isomeric 3-indole analogues displayed Schild potencies similar to those of the parent series shown in Scheme 1. In particular, compound **5g** has equal potency to **5a** against EP2, compound **5h** with one less methoxyl group has equal potency to a previously described 1-indole isomer with two methoxyl derivative TG4-166,[43] indicating that both indole positional isomers are equally active to pursue further. Compound **5j** has about 3-fold less potency to equivalent **5c**. Moreover, incorporation of two fluorine atoms on the indole phenyl ring to block the ortho and para (fifth, seventh) positions to the ring nitrogen (**5i**) maintained EP2 potency of the parent **5a**. This result is consistent with our previous observation, where one fluorine atom at (fifth position) para to indole nitrogen on the phenyl ring yielded an equally potent compound to **5a**.[43] Nonetheless, all of these derivatives **5g**,**h** showed EP2 Schild K_B values less than that of the previous lead compound **5d**. These 3-indole derivatives (**5g**−**j**) also displayed improved selectivity (45- to 80-fold) against DP1 (Table 1). To determine whether indole ring can be replaced with other structurally equivalent rings, a benzofuran derivative **5k** was synthesized starting from 3-bromo-2-methylfuran as shown in Supporting Information Scheme S1. This analogue (**5k**) showed 138-fold reduced potency compared to its indole equivalents **5a** and **5g**. We then synthesized and tested an indazole derivative **6t** (Figure 2), but this derivative completely lost EP2 potency. Moreover, we also examined other scaffolds such as indolin-2-one (**5p**) and phenyethyl and phenylpropyl groups (**5q**, **5r**) (Figure 2). However, these derivatives showed very weak (300- to 1000-fold less) potencies (Table 1). In our earlier study we had shown that a 2-methylpiperidine ring (in

Scheme 2. Synthesis of Isomeric Indole-3 Cinnamic Amide Analogues for SAR Study[a]

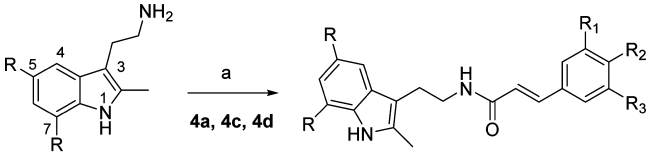

3k. R = H
3l. R = F

5g: R = H, R_1-R_3 = OCH_3
5h: R, R1 = H, R_2-R_3 = OCH_3
5i: R = F, R_1-R_3 = OCH_3
5j: R = H, R_1, R_3 = CH_3, R_2 = F

[a]Reagents and conditions: (a) cinnamic acid derivative (**4a** or **4c** or **4d**), EDCl, DMAP, CH_2Cl_2, 70−80%.

Scheme 3. Synthesis of More Aqueous Soluble First Generation Cinnamic Amide EP2 Antagonists[a]

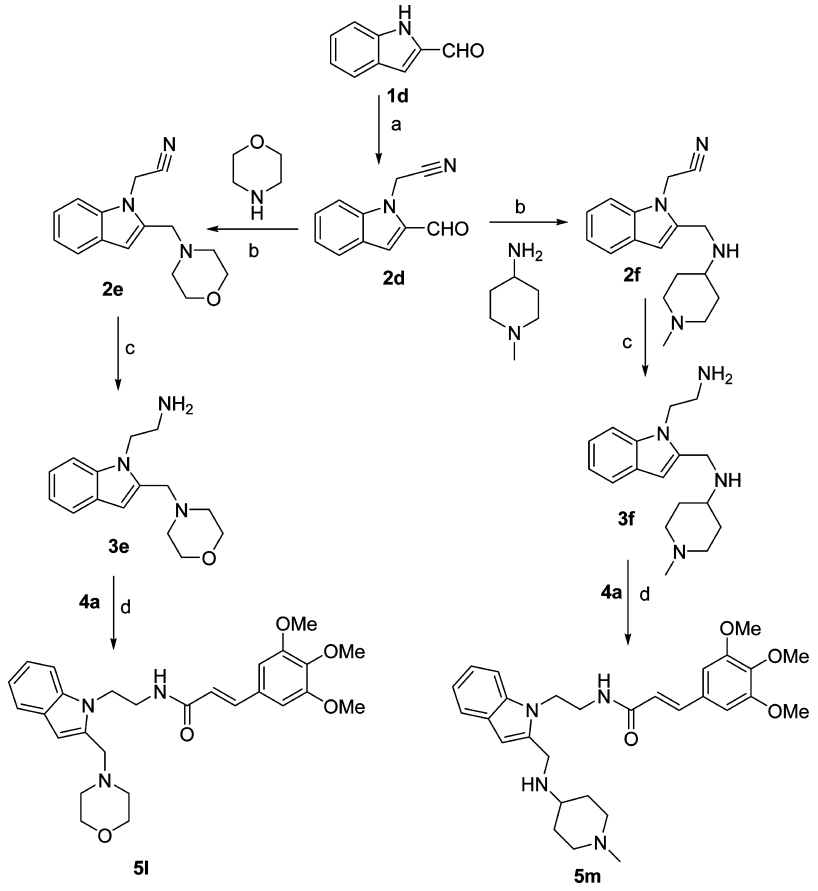

[a]Reagents and conditions: (a) NaH, bromoacetonitrile, DMF, 75%; (b) morpholine or 4-amino-1-methylpiperidine, $Na(OAc)_3BH$, AcOH, 60−75%; (c) LAH, THF, **3e**, 55%, **3f**, 20%; (d) cinnamic acid (**4a**), EDCl, DMAP, CH_2Cl_2, 75%.

dx.doi.org/10.1021/jm5000672 | *J. Med. Chem.* 2014, 57, 4173−4184

Scheme 4. Synthesis of Aqueous Soluble Hydroxyethyl Ether Cinnamic Amide Derivatives[a]

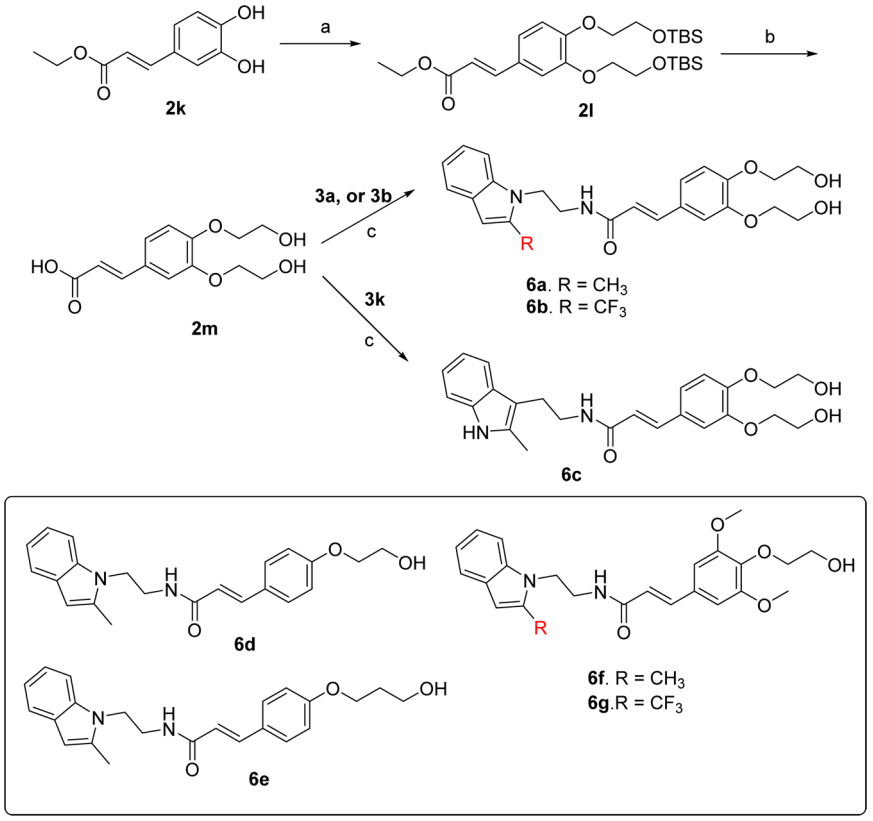

[a]Reagents and conditions: (a) 2-*tert*-butyldimethylsilyloxyethanol, PPh_3, DIAD,THF, reflux, 36 h, 70%; (b) 1 N NaOH, THF, 2 N HCl, 801%; (c) **3a**, **3b**, or **3k**, EDCl, DMAP, DCM/DMF (5:1), 80%.

place of indole ring) derivative **6j** (Figure 2) displayed complete loss of activity.[43] Taken together, these results suggest that the indole (1- or 3-positional isomers) ring is crucial for higher EP2 potency but substitution on the indole rings is allowable.

Although several compounds from Schemes 1 and 2 (**5a–d**, **5g–j**) showed high EP2 potency and improved DP1 selectivity, they displayed poor aqueous solubility (Table 1). We explored two strategies to improve the aqueous solubility in this class of compounds. First, we functionalized the indole ring at second and third positions (see Figure 1 for number illustration) with more polar functional groups that should enhance the solubility of the scaffold. As shown in Scheme 3, the synthesis is initiated with 2-formylindole (**1d**), which on treatment with bromoacetonitrile provided **2d**, which then on reductive amination[49] with morpholine and 4-amino-1-methylpiperidine provided **2e** and **2f**. These compounds were reduced with lithium aluminum hydride to get **3e** and **3f**, which were then coupled to 3,4,5-trimethoxycinnamic acid (**4a**) to provide final products (**5l**, **5m**). Similarly, 3-substituted indoles (**5n–o**) with more solubilizing functional groups were synthesized as shown in Supporting Information Scheme S2. We anticipated that these derivatives **5l–o** could be transformed into their hydrochloride salt (HCl) forms to improve the solubility as needed. Indeed, these derivatives (**5l–o**) and their HCl salts forms (not shown) have improved solubility in the range of 75–180 μM (Table 1) compared to parents **5a** and **5d**, but they failed to show a strong EP2 antagonistic activity at 1 μM (Table 1), suggesting these regions on the indole ring are not flexible for structural modification.

The second strategy that we explored to improve the aqueous solubility of the scaffold **5a** and **5d** is a substitution of methoxyl groups with one or two hydroxyalkyl groups on the phenyl ring. The synthesis of these analogues is shown in Scheme 4. First commercially available 3,4-dihydroxycinnamic acid ethyl ester (**2k**) was subjected to Mitsunobu reaction[50] with 2-*tert*-butyldimethylsilyloxyethanol to get bis-*tert*-butyldimethylsilyloxy ether (**2l**), which on treatment with 1 N NaOH in refluxing tetrahydrofuran and then quenching with 2 N HCl (in one pot) provided precursor acid (**2m**). This acid was coupled individually to indole amine **3a**, **3b**, or **3k** to provide final products (**6a–c**) with two pendent hydroxyethyl ether moieties. As we predicted, compounds **6a** and **6c** have 3- to 5-fold higher aqueous solubility (Table 1) in comparison to parent compound **5a** when measured by nephelometry in PBS buffer in 1% DMSO.[51] Similarly, a trifluoromethylindole compound (**6b**) has shown 2.5-fold higher solubility (67 μM) in comparison to its parent compound **5d** (Table 1). Moreover, we also synthesized several compounds with only one hydroxyethyl ether or hydroxypropropyl ether moieties (**6d–g**). These derivatives also showed about 1.2- to 1.4-fold higher solubility than the parents **5a** and **5d** (Table 1).

Some compounds with improved aqueous solubility have high EP2 potency. For example, compounds **6a**, **6d**, and **6e** displayed similar EP2 potency (Schild K_B of 11.4–13.6 nM). These derivatives are about 5-fold less potent than **5a** but are slightly more potent than **5d**. Among these three, **6a**, a bis-hydroxyethyl ether compound, exhibited 44-fold selectivity to DP1, but monohydroxyethyl ether derivatives **6d**, **6e**, and **6f** displayed <10-fold selectivity (Table 1). Likewise, compound

dx.doi.org/10.1021/jm5000672 | J. Med. Chem. 2014, 57, 4173–4184

Table 1. EP2 Bioactivity, DP1 Selectivity, and Aqueous Solubility of Cinnamic Amide Analogues[a]

	compd	K_B (nM) EP2	DP1	SI (DP1/EP2)	solubility (μM)
5a	TG4-155	2.4	34.5	14.4	45
5b	TG7-23	3.4	83	24	<25
5c	TG7-98	3.4	210	60	<25
5d	TG6-10-1	17.8	166	9.3	27
5e	TG7-2	305	ND	ND	ND
5f	TG7-13	306	ND	ND	ND
5g	TG7-74	2.4	110	45	43
5h	TG7-76	4.9	255	52	41
5i	TG7-96	3.3	175	53	<25
5j	TG7-186	11.3	900	80	<25
5k	TG7-122	333	ND	ND	ND
5l	TG7-6	>1000	ND	ND	91
5m	TG7-9	>1000	ND	ND	180
5n	TG7-21	>1000	ND	ND	75
5o	TG7-138	>1000	ND	ND	110
5p	TG7-109	>1000	ND	ND	ND
5q	TG7-91	>1000	ND	ND	ND
5r	TG7-95	667	ND	ND	ND
5s	TG8-116	>1000	ND	ND	ND
5t	TG7-133	>1000	ND	ND	ND
5u	TG7-89	>1000	ND	ND	ND
5v	TG4-156	214	ND	ND	ND
5w	TG7-149	410	ND	ND	ND
5x	TG7-128	680	ND	ND	ND
5y	TG7-97	>1000	ND	ND	ND
5z	TG7-103	>1000	ND	ND	ND
6a	TG8-4	11.4	505	44	153
6b	TG8-16	260	2820	10	67
6c	TG8-21	41.1	7450	181	235
6d	TG8-23	13.6	108	7.9	68
6e	TG8-32	11.8	67.1	5.6	66
6f	TG8-27	3.7	19.9	5.3	66
6g	TG8-30	58.3	198	3.4	35
6h	TG7-209	340	ND	ND	ND
6i	TG7-273	236	ND	ND	ND
6j	TG-109-1	>1000	ND	ND	ND
6k	TG8-57	84.5	752	8.9	180
6l	TG8-53	74.6	283	3.8	306
6m	TG8-56	137	265	2	90
6n	TG7-291	>1000	ND	ND	ND
6o	TG7-294	>1000	ND	ND	ND
6p	TG8-17-1	>1000	ND	ND	ND
6q	TG4-94-1	16.5	66	4	ND
6r	TG8-117	29.2	ND	ND	ND
6s	TG8-118	13.0	ND	ND	ND
6t	TG8-122	>1000	ND	ND	152

[a]Schild K_B values are calculated using the formula $\log(dr - 1) = \log X_B - \log K_B$, where dr (dose ratio) = fold shift in EC_{50} of PGE_2 by the test compound, X_B is antagonist concentration [1 μM]. K_B value indicates a concentration required to produce a 2-fold rightward shift of PGE_2 concentration–response curve. The values are the mean of two to four independent measurements run in duplicate. The solubility of the compounds is measured in PBS buffer (pH 7.4) with 1% DMSO by nephelometry.[51] ND = not determined.

6c, which showed 17-fold less potency than **5a**, 2.3-fold less than **5d**, showed very high selectivity (180-fold) to DP1. This compound is the second most soluble in this whole class of compounds thus far. Moreover, compound **6f**, which has two extra methoxyl groups in addition to a hydroxyethyl ether unit, has nearly equal EP2 potency to **5a**, but a CF_3 analogue **6g** showed 3.2-fold less potency than its parent **5d** (Table 1). In contrast to bis-hydroxyethyl ether derivatives **6a–c**, the monohydroxyethyl ether derivatives **6d–g** showed a modest selectivity (5- to 8-fold) over DP1 (Table 1).

We also synthesized compounds **6k–m** containing a 2-dimethylaminoethoxy ether group on the phenyl ring as shown in Scheme 5. The qikprop (Schrodinger Inc.) predicted ADME properties (see Supporting Information Table S2) suggest that these derivatives may display similar solubilities (due to basic nitrogen) to hydroxyethyl ethers (**6a–g**) and may show improved metabolic stability and brain penetration properties because the pendent tertiary amine group is masked by hydrophobic methyl groups. Indeed, compounds **6k–m** have enhanced solubility (180, 306, and 90 μM, respectively) (Table 1). However, these derivatives have reduced EP2 potencies (Table 1) in comparison to their hydroxyethyether equivalents **6d–f**. Given their reduced potency and modest selectivity against DP1 (Table 1), they are not tested for liver metabolism and brain-permeation properties. A future study will address whether incorporation these basic amine functionality at meta or ortho positions improves EP2 potency and selectivity against DP1.

In our earlier study,[43] we briefly explored the linker unit for structural modification and learned that extension of two-carbon ethylamino chain (see Figure 1) to three-carbon propylamino chain resulted in 775-fold less EP2 potency, and saturating the double bond of acrylamide as in **5v** (Figure 2) reduced the potency by 90-fold compared with **5a** (Table 1). In the present study, we synthesized compounds with one-carbon methylamino linker such as **5s**,**t** (Figure 2), but these analogues showed complete loss of potency (Table 1). We also synthesized an analogue by reversing the amide (**5u**, Figure 2), which also killed EP2 potency. However, saturation of the double bond and then addition of an amino group (**5w**), or reducing the length of acrylamide to single methylphenyl (**5x**) (Figure 2), reduced the potency by 180- and 160-fold, respectively, in comparison to **5a**. Given the limited availability of synthetic methods to modify the ethylene linker (Figure 1), only two derivatives with a carboxymethyl ester group on the ethylamine linker (**5y**,**z**) have been synthesized, but these compounds were inactive on EP2. Moreover, to determine whether the amide is absolutely essential for EP2 potency, we synthesized an ester analogue **6h** (Figure 2). This analogue showed about 140-fold less potency than **5a**, suggesting that the potency in the scaffold arises not just from the acrylamide in the linker. Furthermore, we synthesized a cyclopropylamide analogue **6i**, which showed 100-fold less potency than **5a**. Taken together, these results suggest an ethylamine linker, one side attached to the indole ring and other side attached to the acrylamide, is optimal for bioactivity, but acrylamide moiety is not solely responsible for the activity; thus, it may be expendable.

To minimize the conformational freedom arising from the ethylamine linker and to minimize the exposure of the linker unit to metabolizing enzymes, we synthesized derivatives with constrained and bulkier internal cyclic rings **6n–p** as shown in Supporting Information Scheme S3. Compounds **6n–p** were inactive suggesting that the acyclic ethylene amide is essential for high EP2 potency. It is worth mentioning that **6n–p** are chiral compounds; we have synthesized only racemic forms,

dx.doi.org/10.1021/jm5000672 | J. Med. Chem. 2014, 57, 4173–4184

Scheme 5. Synthesis of 2-Dimethylaminoalkyl Ether Cinnamic Amide Derivatives[a]

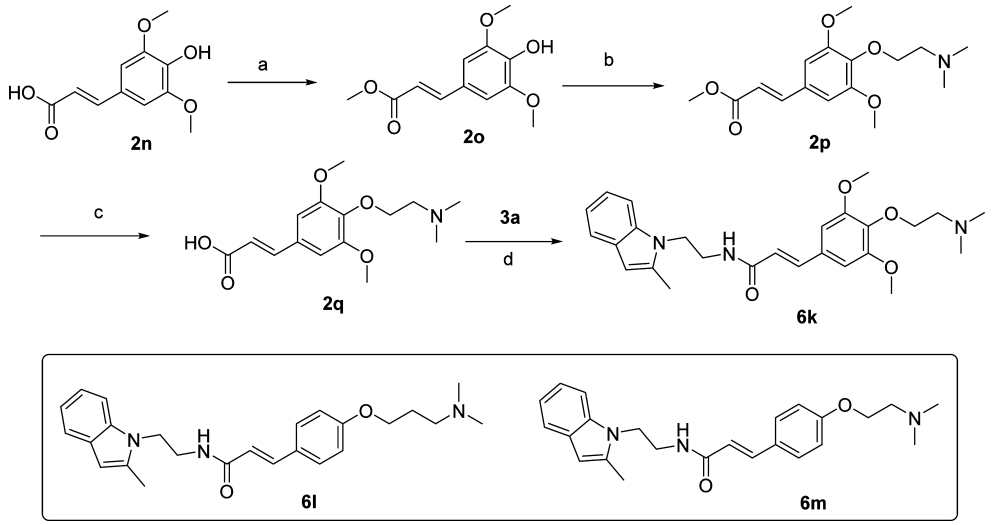

[a]Reagents and conditions: (a) MeOH, H_2SO_4 (drops), reflux, quantitative; (b) dimethylaminoethanol, PPh_3, DIAD, THF, 70%; (c) 1 N NaOH, THF, reflux, quantitative (reagent grade salt); (d) **3a**, EDCl, DMAP, DMF, 70%.

Table 2. EP2 Potency, Selectivity against EP4 and IP Receptors, and Cytotoxicity of Selected EP2 Antagonists[a]

compd	K_B(EP2), nM	K_B(EP4), μM	selective index EP4/EP2	K_B(IP), μM	selective index IP/EP2	cytotoxicity CC_{50}, μM	therapeutic index CC_{50}/K_B(EP2)
5a (TG4-155)	2.4	11.4	4750	62	25800	172	71700
5c (TG7-98)	3.4	41.0	12100	22.5	6630	368	108 000
5d (TG6-10-1)	17.8	11.2	630	8.45	475	81	4550
5g (TG7-74)	2.4	4.3	1790	12.7	5310	59.5	24800
5h (TG7-76)	4.9	1.46	300	42.7	8720	246	50200
5j (TG7-186)	11.3	3.5	310	21.7	1920	317	28000
6a (TG8-4)	11.4	7.13	625	1.57	138	92.3	8100
6c (TG8-21)	41.1	9.5	230	240	5840	126	3060
6d (TG8-23)	13.6	7.58	560	30.0	2200	81.7	6000
6e (TG8-32)	11.8	5.96	505	210	1780	36.6	3100
6f (TG8-27)	3.7	7.49	2020	85.0	23000	43.3	11700
6g (TG8-30)	58.3	7.93	136	95.9	164	31.2	535

[a]EP2, EP4, and IP Schild K_B values are average of two to three independent experiments run in duplicate. CC_{50} values are the average of two measurements run in triplicate. CC_{50} = critical concentration required to kill 50% cells.

and we did not make any effort to make them in enantiomerically enriched form because of their weak or nil potency.

Overall, SAR indicates that in the 1- or 3-indole rings, a CH_3 at second position is optimal for EP2 potency. A small structural change at the second position, for example, a CF_3 group, reduces EP2 potency by 7−18 times (cf. **5a** vs 5d; **5e** vs **6q**). An acrylamide group is optimal for high EP2 potency but may be removed. Modifications to the amide group and to the ethylamine linker reduce or eliminate EP2 potency. But three methoxyl groups on the phenyl ring could be substituted with a variety of other groups to maintain high EP2 potency.

Novel Analogues Show High EP2 Selectivity over Other Prostanoid Receptors. As indicated briefly in the previous section, there are nine prostanoid receptors in the family: DP1, DP2, EP1, EP2, EP3, EP4, FP, IP, and TP. These receptors are widely distributed in organs and cell types and are activated by endogenous prostanoids (PGD_2, PGE_2, PGF_2, PGI_2, and TXA_2). Among these receptors, EP1, EP2, EP3, and EP4 share a common endogenous ligand PGE_2 for their activation. EP2 and EP4 are positively coupled to cAMP signaling, whereas EP3 inhibits cAMP production and EP1 mediates cytosolic Ca^{2+} signaling, suggesting that these receptors could play different, often opposite, roles in pathophysiology.[27−29] On the other hand, although DP1 receptor is not activated by PGE_2, it has the highest structural homology to EP2 and is known to exert proinflammatory effects similar to those of EP2 in certain conditions.[27−29] EP2 receptor also shares a 40% structural homology to the IP receptor. IP receptor activation is shown to play an important role in cardioprotection.[15,17] Thus, it is crucial to establish selectivity for the novel antagonists to EP2 over DP1, EP4, and IP, for preclinical and clinical studies. Previously synthesized first generation analogues[43,44]and several other newly synthesized derivatives showed modest selectivity to DP1 (Table 1). But derivatives **5c**, **5g−j**, **6a**, **6c** showed >44-fold selectivity to EP2 over DP1. So we selected these derivatives for selectivity testing against EP4 and IP receptors. We created cell lines that overexpress EP4 receptors, or IP receptors on C6-glioma cells, and developed a cAMP-derived TR-FRET assay using agonists PGE_2 (for EP4) and iloprost (for IP), similar to EP2 assay (see Experimental Methods for details). The results show that the new analogues display micromolar Schild K_B values for EP4 and IP receptors (Table 2), with high selectivity indexes. For

dx.doi.org/10.1021/jm5000672 | J. Med. Chem. 2014, 57, 4173−4184

Table 3. Liver Microsomal Stability and in Vivo Pharmacokinetic Properties of Selected Compounds[a]

	% of parent compound remaining at 60 min vs T = 0 min				mouse in vivo pharmacokinetics properties				
	human liver microsomes		mouse liver microsomes						
compd	1 μM	10 μM	1 μM	10 μM	route of administration (dose, mg/kg)	C_{max} (ng/mL)	AUC_{last} (h·ng/mL)	$T_{1/2}$ (plasma) (h)	B/P
5a (TG4-155)	0.1	10.6	0.2	4.8	iv (3)	2400 ± 350	749 ± 24	0.45	0.3
					ip (3)	738 ± 207	457 ± 64	0.58	
5c (TG7-98)	20.9	24.0	18.3	13.0	nd	ND	ND	ND	ND
5d (TG6-10-1)	2.3	39.9	2.0	23.1	ip (5)	115 ± 44	453 ± 49	1.6	1.8
					po (10)	248 ± 61	475 ± 60	1.8	1.6
5g (TG7-74)	0.8	5.8	0	0.2	nd	ND	ND	ND	ND
5h (TG7-76)	12.4	18.6	0.2	0.1	nd	ND	ND	ND	ND
5j (TG7-186)	0.4	21.4	0.1	51.7	nd	ND	ND	ND	ND
6a (TG8-4)	16.2	43.8	1.7	8.7	ip (5)	1510 ± 142	1050 ± 58	1.49	<0.1
					po (10)	128 ± 23	197 ± 26	1.44	<0.1
6c (TG8-21)	58.5	70.4	7.1	19.3	ND	ND	ND	ND	ND

[a]Male or female C57Bl/6 mice were used for in vivo pharmacokinetic study. Formulation used: 5% DMA, 50% PEG400, and 45% saline for compound **5a**; 10% DMSO, 50% PEG400, 40% sterile water for **5d**; and 2.5% DMA, 12.5% propylene glycol, and 85% phosphate-buffered saline (pH 7.4) for **6a**. DMA = *N*,*N*-dimethylacetamide. C_{max} is the maximum observed concentration that occurs at T_{max}. $T_{1/2}$ is the terminal half-life. AUC = area under the curve from time zero to the time of the last measurable observation (AUC_{last}). B/P = brain to plasma ratio, calculated from drug concentrations in plasma and brain tissue at 1 and 2 h. ND = not determined.

example, **5c** displayed 12100-fold selectivity against EP4 and over 6000-fold selectivity against IP receptor. Compound **5g** also displayed high selectivity to EP2 over EP4 (1790-fold) and IP (5310-fold). Likewise compounds **5h** and **5j** showed 300- and 310-fold selectivity to EP4 and 8720- and 1920-fold selectivity to IP receptor (Table 2). However, these derivatives showed weak aqueous solubility (<25 μM). Compounds with improved aqueous solubility, for example, **6a**, displayed 625-fold selectivity against EP4 and 138-fold selectivity against IP; **6c** displayed 230-fold selectivity to EP4 and greater than 5000-fold selectivity against IP. Likewise, compounds **6d**−**f** also displayed good selectivity against EP4 and IP receptor (Table 2), but these latter derivatives showed poor selectivity against DP1 (Table 1). Compound **6g** has slightly less selectivity to EP4 (136-fold) and IP (164-fold) (Table 2). We also tested these selective antagonists in a cell viability assay against C6 glioma cells, and these derivatives have insignificant toxicity with in vitro therapeutic indexes over several orders of magnitude (Table 2).

New Selective EP2 Antagonists Show Improved Microsomal Stability. Having several potent and selective EP2 antagonists in hand, we asked whether any of these compounds show improved metabolic stability in human and mouse liver microsomes in comparison to previous lead compound **5d**. Compound **5a**, which showed 0.2% remaining at 60 min (at 1 μM concentration) in mouse liver microsomes, exhibited an in vivo plasma half-life of ∼30 min. Compound **5d** with 2% remaining at 60 min had 1.6 h in vivo plasma half-life in mouse (Table 3), suggesting that in vitro liver metabolism may be correlated to in vivo plasma half-life in this class. Thus, we examined novel compounds that showed enhanced selectivity in comparison to previous lead **5d** for liver microsomal stability. Compound **5c** showed high stability in both liver fractions, but this compound exhibited poor aqueous solubility; thus, it was not selected for further exploration. Likewise, 3-indole isomeric derivatives **5g**−**j** also showed poor stability in liver fractions (Table 3). Interestingly, a 5-fold more aqueous soluble compound **6a** showed nearly similar stability in both liver fractions in comparison to **5d**. Furthermore, compound **6c** which is about 8-fold more soluble than **5d** displayed 3-fold improved stability in mouse liver fractions. It is also more stable in human liver microsomal fractions (Table 3), suggesting that these two compounds are suitable for in vivo pharmacokinetic study.

ADME Characterization and Pharmacokinetic Studies of Selected EP2 Antagonists. We examined a number of these derivatives to estimate their ADME properties by qikprop software (Schrodinger Inc.). As shown in Supporting Information Table S2, compounds **6a**, **6c**, and **6f** possess solubility and permeability properties in the suggested range for 95% of the known drugs. However, because of the free hydroxyl group, they may encounter some resistance in crossing the blood−brain barrier (BBB) because the predicted values for **6a** and **6c** are lower in comparison to **5d**, a compound experimentally determined to be highly brain permeable. Nonetheless, we have selected compound **6a** and subjected it to in vivo pharmacokinetics study in C57Bl6 mice. As shown in Table 3, this compound displayed more than an hour plasma half-life. However, its brain penetration property is poor compared to previous lead **5d** (Table 3), consistent with qikprop predictions (Supporting Information Table S2).

Blood−brain barrier (BBB) is composed of a network of endothelial cells, astroglia, pericytes, and a basal lamina. The capillary of endothelium of the brain is sealed by tight junctions, produced by the interaction of several transmembrane proteins.[52,53] Interaction of these junctional proteins blocks the entry of polar solutes from blood along the paracellular pathways and so denies access to brain interstitial fluid. However, small molecules with less than 500 molecular weight and high lipophilicity can pass through this barrier by passive transport mechanism. Small molecules could also enter into brain by other mechanisms (e.g., active transport).[54,55] Endothelial cells also express a variety of efflux pumps on their surface, which play a role in export of small molecules into brain. Compound **5d** (our earlier lead) and **6a** display <500 molecular weight, but **5d** is more lipophilic than **6a** based on its poor aqueous solubility (Table 1) and predicted log P (Table 2). On the other hand, compound **6a** is more polar (5-fold

dx.doi.org/10.1021/jm5000672 | J. Med. Chem. 2014, 57, 4173−4184

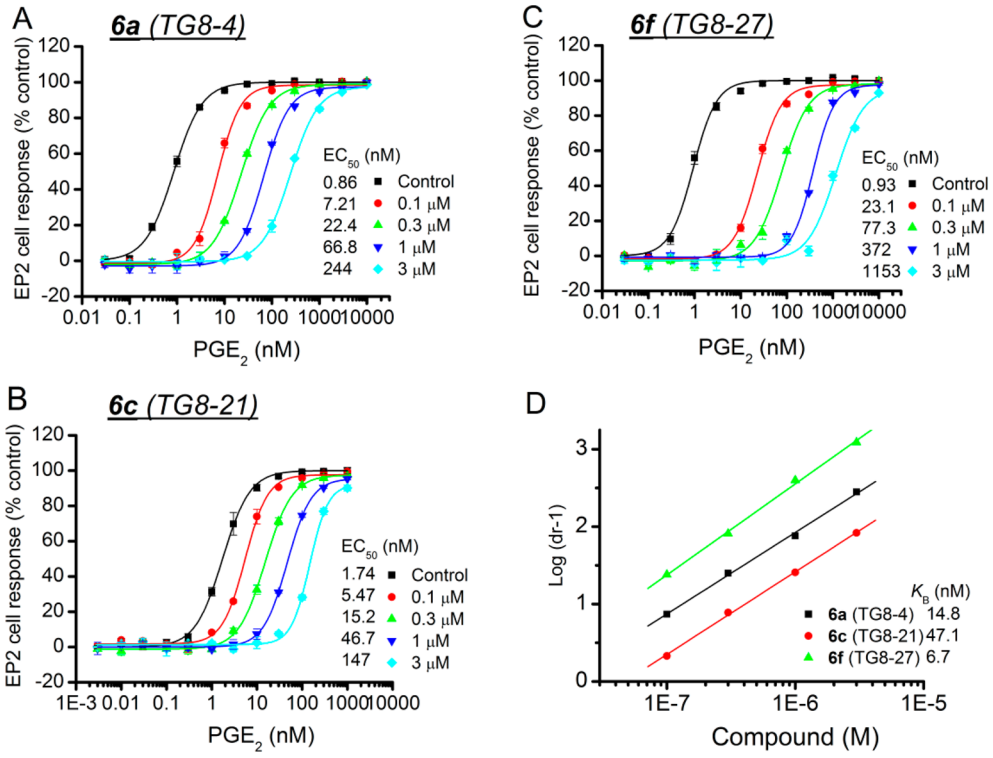

Figure 3. Competitive antagonism of EP2 receptor by novel acrylamide analogues. (A–C) Compounds **6a** (TG8-4), **6c** (TG8-21), and **6f** (TG8-27) inhibited PGE_2-induced human EP2 receptor activation in a concentration dependent manner. (D) Schild regression analysis is performed to determine the modality of antagonism by these compounds. Schild K_B values for each compound are shown in inset of part D. Data were normalized as percentage of maximum response; points represent the mean ± SEM (n = 4). We observed about 1.1- to 1.8-fold higher K_B values from dose–response test in comparison to K_B values derived from single concentration (1 μM) tests (presented in Table 2). These changes are within the limits of assay variability.

more aqueous soluble) with two free hydroxyl groups readily available to form hydrogen bonds. However, we do not yet know whether low levels of **6a** in brain are due to poor passive diffusion or extrusion by efflux pumps. A future study will address this question by synthesis and testing of additional hydroxyl group masked derivatives (e.g., methoxy ethers). Nevertheless, **6a** displayed a 2-fold higher potency and 4-fold higher selectivity against DP1 and 4-fold higher aqueous solubility than **5d**; thus, this compound should be useful for exploring in in vitro and in vivo proof of concept studies in a variety of peripheral disease models where EP2 plays a deleterious role.[56−60]

Novel Analogues Show Competitive Mechanism of Inhibition. We previously demonstrated that compounds **5a** and **5d** and other analogues in this class exhibit a competitive antagonism of EP2.[43,44] All of these derivatives had only methoxyl groups on the phenyl ring. In this study, to determine whether the compounds containing hydroxyethyl ether moieties (**6a−g**) also exhibit a similar mechanism of action, we selected three derivatives **6a**, **6c**, and **6f** and tested them in concentration response against PGE_2 EC_{50} on EP2 receptors. As illustrated in Figure 3D, a linear regression of log(dr − 1) on log X_B with slope of unity characterizes a competitive antagonism. Schild K_B values are derived by the equation log(dr −1) = log X_B − log K_B, where dr = dose ratio (i.e., the fold shift in EC_{50}), X_B is [antagonist], and K_B indicates the antagonist concentration required for a 2-fold rightward shift in the PGE_2 concentration–response curve. A lower K_B value indicates a higher inhibitory potency. The selected three compounds induced a concentration-dependent, parallel rightward shift in the PGE_2 concentration–response curve (Figure 3A–C). Schild regression analyses demonstrated that these compounds have a competitive mechanism of antagonism on EP2 with Schild K_B 14.8 nM for **6a**, 47.1 nM for **6c**, and 6.7 nM for **6f**. Thus, the mechanism is competitive in general for this class of EP2 antagonists presented in this study.

In conclusion, we have synthesized 45 new cinnamic amide EP2 antagonists to optimize the selectivity against DP1 and IP receptors and to improve aqueous solubility and pharmacokinetics properties. Two compounds, namely, **6a** (TG8-4) and **6c** (TG8-21), emerged as selective EP2 antagonists (with 44- to 180-fold selectivity against DP1), with more aqueous solubility (153 and 235 μM) and more stability in vitro in pooled human and mouse liver microsomes in comparison to previous lead compound **5d** (TG6-10-1). But in vivo pharmacokinetics properties still need to be optimized within the class to be useful for in vivo preclinical studies. However, the new analogues **6a** and **6c** could serve as tools for in vitro proof of concept studies.

EXPERIMENTAL METHODS

Chemistry General. Proton NMR spectra were recorded in solvent in $CDCl_3$ on a Varian Inova 400 (400 MHz) instrument. Thin layer chromatography was performed on precoated, aluminum-backed plates (silica gel 60 F_{254}, 0.25 mm thickness) from EM Science and was visualized by UV lamp. Column chromatography was performed with silica gel cartridges on Teledyne-ISCO machine. An Agilent LCMS instrument was used to measure purity of the products. Elemental analyses were performed by Atlantic Microlab Inc. (Norcross, GA). Chemicals and drugs PGE_2, BW245C, iloprost, and rolipram were purchased from Cayman Chemical.

dx.doi.org/10.1021/jm5000672 | J. Med. Chem. 2014, 57, 4173−4184

General Procedure for Synthesis of 2-(2-Substituted-1*H*-indol-1-yl)acetonitriles (2) from Indoles (1).[61] A solution of 2-(trifluoromethyl)-1*H*-indole (**1b**) (0.5 g, 2.7 mmol) in DMF (2.5 mL) was added to a suspension of NaH (160 mg, 1.5 equiv) in DMF (3 mL) at 0 °C, and the resulting reaction mixture was stirred for 30 min. Then bromoacetonitrile (0.27 mL, 1.5 equiv) in DMF (2.5 mL) was introduced into the above mixture at 0 °C, and then the mixture was brought to room temperature overnight. Water (20 mL) was added to quench the reaction. Then the product was extracted with ethyl ether (30 mL × 3). Organics were washed with water, brine, dried over Na_2SO_4, and concentrated. The crude mass on silica gel chromatography, eluting with 0−10% ethyl acetate, furnished **2b** (865 mg, 71% yield; 85% based on recovered starting material).

*2-(2-Trifluoromethyl-1H-indol-1-yl)acetonitrile (**2b**).* ^{1}H NMR ($CDCl_3$): δ 7.70 (d, J = 8 Hz, 1H), 7.44 (m, 2H), 7.28 (t × d, J = 7.2, 1.6 Hz, 1H), 7.04 (s, 1H), 5.1 (s, 2H). LCMS (ESI): >95% purity at λ = 254 nm. MS m/z, 225 $[M + H]^+$. See Supporting Information for synthesis and characterization data for compounds **2a** and **2c−h**.

General Procedure for Synthesis 2-(2-Substituted-1*H*-indol-1-yl)ethanamines (3) from Acetonitriles (2). To a solution of **2b** (855 mg, 3.81 mmol) in THF (30 mL) was added LAH (1 M, 9.54 mmol, 2.5 equiv), dropwise at 0 °C, and the resulting reaction mixture was brought to room temperature overnight. Methanol (2 mL) was slowly added to quench the reaction at −78 °C, followed by 1 N NaOH (3 mL) at room temperature. The product was extracted with ethyl ether (30 mL × 3). Organics were washed with water, brine and dried over Na_2SO_4 and concentrated. The crude mass was subjected to silica gel chromatography, eluting with 0−5% methanol in dichloromethane to provide **3b** (490 mg, 56% yield).

*2-(2-(Trifluoromethyl)-1H-indol-1-yl)ethanamine (**3b**).* ^{1}H NMR ($CDCl_3$): δ 7.66 (d, J = 8 Hz, 1H), 7.44 (dd, J = 8.4, 0.8 Hz, 1H), 7.34 (t × d, J = 7.6, 0.8 Hz, 1H), 7.17 (t × d, J = 7.4, 1.2 Hz, 1H) 6.94 (s, 1H), 4.28 (t, J = 6.8 Hz, 2H) 3.12 (t, J = 6.8 Hz, 2H) 2.45 (s, 3H). LCMS (ESI): >97% purity at λ = 254 nm. MS m/z, 229 $[M + H]^+$. See Supporting Information for synthesis and characterization data for **3a** and **3c−h**.

General Procedures for Synthesis of Cinnamic Amide Final Products. To a solution of **3b** (480 mg, 2.1 mmol) in dichloromethane (10 mL) were added (*E*)-3-(3,4,5-trimethoxyphenyl)acrylic acid (**4a**) (504 mg, 1 equiv), 1-ethyl-3-(3-(dimethylamino)propyl)-carbodiimide hydrochloride (EDCI) (523 mg, 1.3 equiv), and *N*,*N*-dimethylaminopyridine (10 mg), and resulting reaction mixture was stirred at room temperature for 8 h. The reaction was quenched with water (10 mL), and the product was extracted with ethyl acetate (20 mL × 3). Organics were washed with 1% HCl (10 mL), saturated $NaHCO_3$ (10 mL), water (20 mL), brine solution (20 mL) and dried over Na_2SO_4. The crude product was purified by silica gel chromatography, eluting with 0−35% ethyl acetate in hexane to provide **5d** (700 mg, 74% yield).

*(E)-N-(2-(2-(Trifluoromethyl)-1H-indol-1-yl)ethyl)-3-(3,4,5-trimethoxyphenyl)acrylamide (**5d**).* ^{1}H NMR ($CDCl_3$): δ 7.59 (d, J = 8 Hz, 1H), 7.54 (d, J = 8.4, Hz, 1H), 7.50 (d, J = 15.2 Hz, 1H), 7.27 (q, J = 7.2 Hz, 1H), 7.1 (t, J = 7. 2 Hz, 1H), 6.89 (s, 1H), 6. 63 (s, 2H), 6.4 (t, J = 6 Hz, 1H), 6. 25 (d, J = 15.2 Hz, 1H), 4.4 (t, J = 6.4 Hz, 1H), 3.8 (s, 3H), 3.76 (s, 6H), 3.69 (q, J = 6.4 Hz, 2H). LCMS (ESI): >95% purity at λ = 254 nm. MS m/z, 449 $[M + H]^+$. Anal. Calcd for $C_{23}H_{23}F_3N_2O_4$: C, 61.60; H, 5.17; N, 6.25. Found: C, 61.34; H, 5.10; N, 6.16. See Supporting Information for characterization of **5a−c,e−z**.

General Synthesis for 2-Hydroxyethyl- Or 2-Dimethylaminoethylcinnamic Acids. *Step 1.* To a solution of ethyl-3,4-dihydroxycinnamate (**2k**) (460 mg, 2.21 mmol), 2-*tert*-butyldimethylsilyloxyethanol (2 mL, 9.52 mmol 4.3 equiv), and triphenylphosphine (3.43 g, 13 mmol, 5.8 mmol) in THF (40 mL) was added diisopropyl azodicarboxylate (2.4 mL, 12 mmol, 5.3 equiv) dropwise at 0 °C. Then the resulting solution was refluxed for 36 h. The volatiles were removed under vacuum and the crude product was subjected to silica gel chromatography, eluting with 0−20% ethyl acetate in hexane to furnish **2l** (775 mg, 67%).

*Ethyl (E)-3-(3,4-Bis(2-((tert-butyldimethylsilyl)oxy)ethoxy)-phenyl)acrylate (**2l**).* ^{1}H NMR ($CDCl_3$): δ 7.60 (d, J = 15.6 Hz, 1H), 7.07 (dd, J = 6.8, 1.6 Hz, 1H), 7.04 (d, J = 2 Hz, 1H), 6.87 (d, J = 8.4 Hz, 1H), 6.26 (d, J = 16 Hz, 1H) 4.24 (q, J = 6.8 Hz, 2H), 4.07 (q, J = 5.6 Hz, 4H), 3.97 (t, J = 5.6 Hz, 4H), 1.30 (t, J = 7.2 Hz, 3H), 0.88 (two singlets, 18H), 0.08 (two singlets, 12H). LCMS (ESI): >95% purity at λ = 254 nm. MS m/z, 525 $[M + H]^+$.

Step 2. To a solution of **2l** (375 mg, 0.71 mmol) in THF (10 mL) was added 1 N NaOH (2.13 mL, 2.13 mmol, 3 equiv), and the resulting reaction was refluxed for 48 h. The reaction mixture was cooled and neutralized with 1 N HCl (10 mL) to pH 4. Then the product was extracted with ethyl acetate (25 mL × 3). Organics were dried over Na_2SO_4 and concentrated to dryness under vacuum to furnish **2m** (190 mg, quantitative yield), which was used for next step without further purification.

*(E)-3-(3,4-Bis(2-hydroxyethoxy)phenyl)acrylic Acid (**2m**).* ^{1}H NMR (DMSO-d_6): δ 12.0 (bs, 1H), 7.46 (d, J = 15.6 Hz, 1H), 7.29 (d, J = 2 Hz, 1H), 7.14 (m, 1H), 6.96 (d, J = 8 Hz, 1H), 6.38 (d, J = 16 Hz, 1H) 4.0 (m, 4H), 3.68 (bs, 4H). LCMS (ESI): >95% purity at λ = 254 nm. MS m/z, 267 $[M - H]$. See Supporting Information for synthesis and characterization for other carboxylic acid derivatives **2o−q**.

*(E)-3-(3,4-Bis(2-hydroxyethoxy)phenyl)-N-(2-(2-methyl-1H-indol-1-yl)ethyl)acrylamide (**6a**, TG8-4).* This compound was prepared from **2m** and **3a** in 80% yield by the method described for **5d**. ^{1}H NMR ($CDCl_3$): δ 7.46 (d, J = 8.8 Hz, 1H), 7.43 (d, J = 16 Hz, 1H), 7.26 (d, J = 9.6 Hz, 1H), 7.07 (t, J = 6.8 Hz, 1H), 7.04 (t × d, J = 8.4, 2 Hz, 2H), 6.81 (d, J = 8 Hz, 1H), 6.12 (d, J = 15.6 Hz, 1H), 4.25 (t, J = 6 Hz, 2H), 4.04 (q, J = 4 Hz, 4H), 3.87 (q, J = 4.4 Hz, 4H), 3.62 (t, J = 5.6 Hz, 2H), 2.34 (s, 3H). LCMS (ESI): >97% purity at λ = 254 nm. MS m/z, 425 $[M + H]^+$. HRFABMS: calcd for $C_{24}H_{28}N_2O_5Na$, 447.189 04; found 447.189 76.

*(E)-3-(3,4-Bis(2-hydroxyethoxy)phenyl)-N-(2-(2-methyl-1H-indol-3-yl)ethyl)acrylamide (**6c**, TG8-21).* This compound was prepared from **2m** and **3k** in 80% yield by the method described for **5d**. ^{1}H NMR ($CDCl_3$ + MeOH-d_4): δ 7.41 (d, J = 7.2 Hz, 1H), 7.34 (d, J = 15.6 Hz, 1H), 7.19 (d × t, J = 8.4, 0.8 Hz, 1H), 6.92 (m, 4H), 6.77 (d, J = 8 Hz, 1H), 6.10 (d, J = 16 Hz, 1H), 3. 99 (t, J = 4 Hz, 4H), 3.81 (q, J = 3.6 Hz, 4H), 3.48 (t, J = 6.8 Hz, 2H), 2.87 (t, J = 7.2 Hz, 2H), 2.27 (s, 3H). LCMS (ESI): >97% purity at λ = 254 nm. MS m/z, 425 $[M + H]^+$. HRFABMS calcd for $C_{24}H_{28}N_2O_5Na$, 447.189 04; found 447.188 89. See Supporting Information for synthesis and characterization data for remaining compounds **6b,d−p**.

Bioactivity Testing. *Cell Culture.* The rat C6 glioma (C6G) cells stably expressing human DP1, EP2, EP4, or IP receptors were created in the laboratory[43,44,48] and grown in Dulbecco's modified Eagle medium (DMEM) (Invitrogen) supplemented with 10% (v/v) fetal bovine serum (FBS) (Invitrogen), 100 U/mL penicillin and 100 μg/mL streptomycin (Invitrogen), and 0.5 mg/mL G418 (Invitrogen).

Cell-Based cAMP Assay. Intracellular cAMP was measured with a cell-based homogeneous time-resolved fluorescence resonance energy transfer (TR-FRET) method (Cisbio Bioassays), as previously described.[43,44] The assay is based on generation of a strong FRET signal upon the interaction of two molecules, an anti-cAMP antibody coupled to a FRET donor (cryptate), and cAMP coupled to a FRET acceptor (d2). Endogenous cAMP produced by cells competes with labeled cAMP for binding to the cAMP antibody and thus reduces the FRET signal. Cells stably expressing human DP1, EP2, EP4, or IP receptors were seeded into 384-well plates in 30 μL of complete medium (4000 cells/well) and grown overnight. The medium was carefully withdrawn, and 10 μL of Hanks' buffered salt solution (HBSS) (Hyclone) containing 20 μM rolipram was added into the wells to block phosphodiesterases. The cells were incubated at room temperature for 0.5−1 h and then treated with vehicle or test compound for 10 min before addition of increasing concentrations of appropriate agonist: BW245C for DP1, PGE_2 for EP2 and EP4, or iloprost for IP. The cells were incubated at room temperature for 40 min and then lysed in 10 μL of lysis buffer containing the FRET acceptor cAMP-d2, and 1 min later another 10 μL of lysis buffer with anti-cAMP-cryptate was added. After a 60−90 min incubation at room temperature, the FRET signal was measured by an Envision 2103 multilabel plate reader (PerkinElmer Life Sciences) with a laser

dx.doi.org/10.1021/jm5000672 | J. Med. Chem. 2014, 57, 4173−4184

excitation at 337 nm and dual emissions at 665 and 590 nm for d2 and cryptate (50 μs delay), respectively. The FRET signal was expressed as (F665/F590) × 10^4.

■ ASSOCIATED CONTENT

Supporting Information

Synthesis schemes for compounds **5k**,**o**,**p**, and **6n**−**p**; a table of the reagents and reaction conditions tested to improve yield of starting materials **3** from **2**; a table of qikprop calculations on selected compounds; NMR and MS characterization data for remaining compounds. This material is available free of charge via the Internet at http://pubs.acs.org.

■ AUTHOR INFORMATION

Corresponding Author

*Phone: +1-404-727-7393. Fax: +1-404-727-0365. E-mail: tganesh@emory.edu.

Author Contributions

T.G. and R.D. designed the research. T.G., J.J., and M.-S.Y. performed the research. T.G. wrote the manuscript. R.D. helped with the writing.

Notes

The authors declare no competing financial interest.

■ ACKNOWLEDGMENTS

This work was supported by Alzheimer's Drug Discovery Foundation (T.G.), NIH/NINDS Grants K99/R00NS082379 (to J.J.) and U01NS058158 (to R.D.), NARSAD Young Investigator Grant (to J.J.), and the Epilepsy Foundation (to J.J.).

■ REFERENCES

(1) Akiyama, H.; Barger, S.; Barnum, S.; Bradt, B.; Bauer, J.; Cole, G. M.; Cooper, N. R.; Eikelenboom, P.; Emmerling, M.; Fiebich, B. L.; Finch, C. E.; Frautschy, S.; Griffin, W. S.; Hampel, H.; Hull, M.; Landreth, G.; Lue, L.; Mrak, R.; Mackenzie, I. R.; McGeer, P. L.; O'Banion, M. K.; Pachter, J.; Pasinetti, G.; Plata-Salaman, C.; Rogers, J.; Rydel, R.; Shen, Y.; Streit, W.; Strohmeyer, R.; Tooyoma, I.; Van Muiswinkel, F. L.; Veerhuis, R.; Walker, D.; Webster, S.; Wegrzyniak, B.; Wenk, G.; Wyss-Coray, T. Inflammation and Alzheimer's disease. *Neurobiol. Aging* **2000**, *21*, 383−421.

(2) Heneka, M. T.; O'Banion, M. K. Inflammatory processes in Alzheimer's disease. *J. Neuroimmunol.* **2007**, *184*, 69−91.

(3) McGeer, P. L.; McGeer, E. G. Inflammatory processes in amyotrophic lateral sclerosis. *Muscle Nerve* **2002**, *26*, 459−470.

(4) Nagamoto-Combs, K.; McNeal, D. W.; Morecraft, R. J.; Combs, C. K. Prolonged microgliosis in the rhesus monkey central nervous system after traumatic brain injury. *J. Neurotrauma* **2007**, *24*, 1719−1742.

(5) Przedborski, S. Inflammation and Parkinson's disease pathogenesis. *Mov. Disord.* **2010**, *25* (Suppl.1), S55−S57.

(6) Ramlackhansingh, A. F.; Brooks, D. J.; Greenwood, R. J.; Bose, S. K.; Turkheimer, F. E.; Kinnunen, K. M.; Gentleman, S.; Heckemann, R. A.; Gunanayagam, K.; Gelosa, G.; Sharp, D. J. Inflammation after trauma: microglial activation and traumatic brain injury. *Ann. Neurol.* **2011**, *70*, 374−383.

(7) Vezzani, A.; Aronica, E.; Mazarati, A.; Pittman, Q. J. Epilepsy and brain inflammation. *Exp. Neurol.* **2013**, *244*, 11−21.

(8) Vezzani, A.; French, J.; Bartfai, T.; Baram, T. Z. The role of inflammation in epilepsy. *Nat. Rev. Neurol.* **2011**, *7*, 31−40.

(9) Ho, L.; Pieroni, C.; Winger, D.; Purohit, D. P.; Aisen, P. S.; Pasinetti, G. M. Regional distribution of cyclooxygenase-2 in the hippocampal formation in Alzheimer's disease. *J. Neurosci. Res.* **1999**, *57*, 295−303.

(10) Lucas, S. M.; Rothwell, N. J.; Gibson, R. M. The role of inflammation in CNS injury and disease. *Br. J. Pharmacol.* **2006**, *147* (Suppl. 1), S232−S240.

(11) Minghetti, L. Role of inflammation in neurodegenerative diseases. *Curr. Opin. Neurol.* **2005**, *18*, 315−321.

(12) Pasinetti, G. M.; Aisen, P. S. Cyclooxygenase-2 expression is increased in frontal cortex of Alzheimer's disease brain. *Neuroscience* **1998**, *87*, 319−324.

(13) Cannon, G. W.; Caldwell, J. R.; Holt, P.; McLean, B.; Seidenberg, B.; Bolognese, J.; Ehrich, E.; Mukhopadhyay, S.; Daniels, B. Rofecoxib, a specific inhibitor of cyclooxygenase 2, with clinical efficacy comparable with that of diclofenac sodium: results of a one-year, randomized, clinical trial in patients with osteoarthritis of the knee and hip. Rofecoxib Phase III Protocol 035 Study Group. *Arthritis Rheum.* **2000**, *43*, 978−987.

(14) Clemett, D.; Goa, K. L. Celecoxib: a review of its use in osteoarthritis, rheumatoid arthritis and acute pain. *Drugs* **2000**, *59*, 957−980.

(15) Abraham, N. S.; El-Serag, H. B.; Hartman, C.; Richardson, P.; Deswal, A. Cyclooxygenase-2 selectivity of non-steroidal anti-inflammatory drugs and the risk of myocardial infarction and cerebrovascular accident. *Aliment. Pharmacol. Ther.* **2007**, *25*, 913−924.

(16) Egan, K. M.; Lawson, J. A.; Fries, S.; Koller, B.; Rader, D. J.; Smyth, E. M.; FitzGerald, G. A. COX-2-derived prostacyclin confers atheroprotection on female mice. *Science* **2004**, *306*, 1954−1957.

(17) Grosser, T.; Fries, S.; FitzGerald, G. A. Biological basis for the cardiovascular consequences of COX-2 inhibition: therapeutic challenges and opportunities. *J. Clin. Invest.* **2006**, *116*, 4−15.

(18) Grosser, T.; Yu, Y.; Fitzgerald, G. A. Emotion recollected in tranquility: lessons learned from the COX-2 saga. *Annu. Rev. Med.* **2010**, *61*, 17−33.

(19) Aisen, P. S.; Schafer, K. A.; Grundman, M.; Pfeiffer, E.; Sano, M.; Davis, K. L.; Farlow, M. R.; Jin, S.; Thomas, R. G.; Thal, L. J. Effects of rofecoxib or naproxen vs placebo on Alzheimer disease progression: a randomized controlled trial. *JAMA, J. Am. Med. Assoc.* **2003**, *289*, 2819−2826.

(20) Akula, K. K.; Dhir, A.; Kulkarni, S. K. Rofecoxib, a selective cyclooxygenase-2 (COX-2) inhibitor increases pentylenetetrazol seizure threshold in mice: possible involvement of adenosinergic mechanism. *Epilepsy Res.* **2008**, *78*, 60−70.

(21) Breitner, J. C.; Baker, L. D.; Montine, T. J.; Meinert, C. L.; Lyketsos, C. G.; Ashe, K. H.; Brandt, J.; Craft, S.; Evans, D. E.; Green, R. C.; Ismail, M. S.; Martin, B. K.; Mullan, M. J.; Sabbagh, M.; Tariot, P. N. Extended results of the Alzheimer's disease anti-inflammatory prevention trial. *Alzheimer's Dementia* **2011**, *7*, 402−411.

(22) Dhir, A.; Naidu, P. S.; Kulkarni, S. K. Effect of naproxen, a non-selective cyclo-oxygenase inhibitor, on pentylenetetrazol-induced kindling in mice. *Clin. Exp. Pharmacol. Physiol.* **2005**, *32*, 574−584.

(23) Holtman, L.; van Vliet, E. A.; Edelbroek, P. M.; Aronica, E.; Gorter, J. A. Cox-2 inhibition can lead to adverse effects in a rat model for temporal lobe epilepsy. *Epilepsy Res.* **2010**, *91*, 49−56.

(24) Holtman, L.; van Vliet, E. A.; van Schaik, R.; Queiroz, C. M.; Aronica, E.; Gorter, J. A. Effects of SC58236, a selective COX-2 inhibitor, on epileptogenesis and spontaneous seizures in a rat model for temporal lobe epilepsy. *Epilepsy Res.* **2009**, *84*, 56−66.

(25) Jung, K. H.; Chu, K.; Lee, S. T.; Kim, J.; Sinn, D. I.; Kim, J. M.; Park, D. K.; Lee, J. J.; Kim, S. U.; Kim, M.; Lee, S. K.; Roh, J. K. Cyclooxygenase-2 inhibitor, celecoxib, inhibits the altered hippocampal neurogenesis with attenuation of spontaneous recurrent seizures following pilocarpine-induced status epilepticus. *Neurobiol. Dis.* **2006**, *23*, 237−246.

(26) Polascheck, N.; Bankstahl, M.; Loscher, W. The COX-2 inhibitor parecoxib is neuroprotective but not antiepileptogenic in the pilocarpine model of temporal lobe epilepsy. *Exp. Neurol.* **2010**, *224*, 219−233.

(27) Breyer, R. M.; Bagdassarian, C. K.; Myers, S. A.; Breyer, M. D. Prostanoid receptors: subtypes and signaling. *Annu. Rev. Pharmacol. Toxicol.* **2001**, *41*, 661−690.

(28) Hirata, T.; Narumiya, S. Prostanoid receptors. *Chem. Rev.* **2011**, *111*, 6209−6230.
(29) Narumiya, S.; Sugimoto, Y.; Ushikubi, F. Prostanoid receptors: structures, properties, and functions. *Physiol. Rev.* **1999**, *79*, 1193−1226.
(30) Ganesh, T. Prostanoid receptor EP2 as a therapeutic target. *J. Med. Chem.* [Online early access]. DOI: 10.1021/jm401431x. Published Online: Nov 26, **2013**.
(31) Jiang, J.; Dingledine, R. Prostaglandin receptor EP2 in the crosshairs of anti-inflammation, anti-cancer, and neuroprotection. *Trends. Pharmacol. Sci.* **2013**, *34*, 413−423.
(32) Fujino, H.; Salvi, S.; Regan, J. W. Differential regulation of phosphorylation of the cAMP response element-binding protein after activation of EP2 and EP4 prostanoid receptors by prostaglandin E2. *Mol. Pharmacol.* **2005**, *68*, 251−259.
(33) Regan, J. W. EP2 and EP4 prostanoid receptor signaling. *Life Sci.* **2003**, *74*, 143−153.
(34) Bos, J. L. Epac: a new cAMP target and new avenues in cAMP research. *Nat. Rev. Mol. Cell Biol.* **2003**, *4*, 733−738.
(35) Quan, Y.; Jiang, J.; Dingledine, R. EP2 receptor signaling pathways regulate classical activation of microglia. *J. Biol. Chem.* **2013**, *288*, 9293−9302.
(36) de Rooij, J.; Zwartkruis, F. J.; Verheijen, M. H.; Cool, R. H.; Nijman, S. M.; Wittinghofer, A.; Bos, J. L. Epac is a Rap1 guanine-nucleotide-exchange factor directly activated by cyclic AMP. *Nature* **1998**, *396*, 474−477.
(37) Liang, X.; Wang, Q.; Hand, T.; Wu, L.; Breyer, R. M.; Montine, T. J.; Andreasson, K. Deletion of the prostaglandin E2 EP2 receptor reduces oxidative damage and amyloid burden in a model of Alzheimer's disease. *J. Neurosci.* **2005**, *25*, 10180−10187.
(38) Jin, J.; Shie, F. S.; Liu, J.; Wang, Y.; Davis, J.; Schantz, A. M.; Montine, K. S.; Montine, T. J.; Zhang, J. Prostaglandin E2 receptor subtype 2 (EP2) regulates microglial activation and associated neurotoxicity induced by aggregated alpha-synuclein. *J. Neuroinflammation* **2007**, *4*, 2.
(39) Liang, X.; Wang, Q.; Shi, J.; Lokteva, L.; Breyer, R. M.; Montine, T. J.; Andreasson, K. The prostaglandin E2 EP2 receptor accelerates disease progression and inflammation in a model of amyotrophic lateral sclerosis. *Ann. Neurol.* **2008**, *64*, 304−314.
(40) Montine, T. J.; Milatovic, D.; Gupta, R. C.; Valyi-Nagy, T.; Morrow, J. D.; Breyer, R. M. Neuronal oxidative damage from activated innate immunity is EP2 receptor-dependent. *J. Neurochem.* **2002**, *83*, 463−470.
(41) Shie, F. S.; Breyer, R. M.; Montine, T. J. Microglia lacking E prostanoid receptor subtype 2 have enhanced Abeta phagocytosis yet lack Abeta-activated neurotoxicity. *Am. J. Pathol.* **2005**, *166*, 1163−1172.
(42) af Forselles, K. J.; Root, J.; Clarke, T.; Davey, D.; Aughton, K.; Dack, K.; Pullen, N. In vitro and in vivo characterization of PF-04418948, a novel, potent and selective prostaglandin EP(2) receptor antagonist. *Br. J. Pharmacol.* **2011**, *164*, 1847−1856.
(43) Jiang, J.; Ganesh, T.; Du, Y.; Quan, Y.; Serrano, G.; Qui, M.; Speigel, I.; Rojas, A.; Lelutiu, N.; Dingledine, R. Small molecule antagonist reveals seizure-induced mediation of neuronal injury by prostaglandin E2 receptor subtype EP2. *Proc. Natl. Acad. Sci. U.S.A.* **2012**, *109*, 3149−3154.
(44) Jiang, J.; Quan, Y.; Ganesh, T.; Pouliot, W. A.; Dudek, F. E.; Dingledine, R. Inhibition of the prostaglandin receptor EP2 following status epilepticus reduces delayed mortality and brain inflammation. *Proc. Natl. Acad. Sci. U.S.A.* **2013**, *110*, 3591−3596.
(45) Sugimoto, Y.; Narumiya, S. Prostaglandin E receptors. *J. Biol. Chem.* **2007**, *282*, 11613−11617.
(46) Jiang, J.; Dingledine, R. Role of prostaglandin receptor EP2 in the regulations of cancer cell proliferation, invasion, and inflammation. *J. Pharmacol. Exp. Ther.* **2013**, *344*, 360−367.
(47) Hagmann, W. K. The many roles for fluorine in medicinal chemistry. *J. Med. Chem.* **2008**, *51*, 4359−4369.
(48) Jiang, J.; Ganesh, T.; Du, Y.; Thepchatri, P.; Rojas, A.; Lewis, I.; Kurtkaya, S.; Li, L.; Qui, M.; Serrano, G.; Shaw, R.; Sun, A.; Dingledine, R. Neuroprotection by selective allosteric potentiators of the EP2 prostaglandin receptor. *Proc. Natl. Acad. Sci. U.S.A.* **2010**, *107*, 2307−2312.
(49) Baxter, E. W.; Reitz, A. B. Reductive aminations of carbonyl compounds with borohydride and borane reducing agents. *Org. React.* **2002**, *59*, 1−70.
(50) Mitsunobu, O. The use of diethyl azodicarboxylate and triphenylphosphine in synthesis and transformation of natural-products. *Synthesis* **1981**, 1−28.
(51) Bevan, C. D.; Lloyd, R. S. A high-throughput screening method for the determination of aqueous drug solubility using laser nephelometry in microtiter plates. *Anal. Chem.* **2000**, *72*, 1781−1787.
(52) Alavijeh, M. S.; Chishty, M.; Qaiser, M. Z.; Palmer, A. M. Drug metabolism and pharmacokinetics, the blood−brain barrier, and central nervous system drug discovery. *NeuroRx* **2005**, *2*, 554−571.
(53) Pardridge, W. M. The blood−brain barrier: bottleneck in brain drug development. *NeuroRx* **2005**, *2*, 3−14.
(54) Gabathuler, R. Approaches to transport therapeutic drugs across the blood−brain barrier to treat brain diseases. *Neurobiol. Dis.* **2010**, *37*, 48−57.
(55) Loscher, W.; Potschka, H. Blood−brain barrier active efflux transporters: ATP-binding cassette gene family. *NeuroRx* **2005**, *2*, 86−98.
(56) Banu, S. K.; Lee, J.; Speights, V. O., Jr.; Starzinski-Powitz, A.; Arosh, J. A. Selective inhibition of prostaglandin E2 receptors EP2 and EP4 induces apoptosis of human endometriotic cells through suppression of ERK1/2, AKT, NFkappaB, and beta-catenin pathways and activation of intrinsic apoptotic mechanisms. *Mol. Endocrinol.* **2009**, *23*, 1291−1305.
(57) Donnini, S.; Finetti, F.; Solito, R.; Terzuoli, E.; Sacchetti, A.; Morbidelli, L.; Patrignani, P.; Ziche, M. EP2 prostanoid receptor promotes squamous cell carcinoma growth through epidermal growth factor receptor transactivation and iNOS and ERK1/2 pathways. *FASEB J.* **2007**, *21*, 2418−2430.
(58) Honda, T.; Segi-Nishida, E.; Miyachi, Y.; Narumiya, S. Prostacyclin-IP signaling and prostaglandin E2-EP2/EP4 signaling both mediate joint inflammation in mouse collagen-induced arthritis. *J. Exp. Med.* **2006**, *203*, 325−335.
(59) Sheibanie, A. F.; Khayrullina, T.; Safadi, F. F.; Ganea, D. Prostaglandin E2 exacerbates collagen-induced arthritis in mice through the inflammatory interleukin-23/interleukin-17 axis. *Arthritis Rheum.* **2007**, *56*, 2608−2619.
(60) Sung, Y. M.; He, G.; Hwang, D. H.; Fischer, S. M. Overexpression of the prostaglandin E2 receptor EP2 results in enhanced skin tumor development. *Oncogene* **2006**, *25*, 5507−5516.
(61) Roy, S.; Eastman, A.; Gribble, G. W. Synthesis of *N*-alkyl substituted bioactive indolocarbazoles related to Go6976. *Tetrahedron* **2006**, *62*, 7838−7845.